European Journal of Neuroscience, Vol. 22, pp. 2325–2331, 2005

Tectal neurons signal impending collision of looming objects in the pigeon

Le-Qing Wu, Yu-Qiong Niu, Jin Yang and Shu-Rong Wang
Laboratory for Visual Information Processing, Institute of Biophysics, Chinese Academy of Sciences, 15 Datun Road, Beijing 100101, People's Republic of China

Keywords: optic tectum, receptive field, tectopontine system, time-to-collision, visual system

Abstract

Although the optic tectum in non-mammals and its mammalian homolog, the superior colliculus, are involved in avoidance behaviors, whether and how tectal neurons respond to an object approaching on a collision course towards the animal remain unclear. Here we show by single unit recording that there exist three classes of looming-sensitive neurons in the pigeon tectal layer 13, which sends looming information to the nucleus rotundus or to the tectopontine system. The response onset time of tau cells is approximately constant whereas that for rho and eta cells depends on the square root of the diameter/velocity ratio of objects looming towards the animal, the cardioacceleration of which is also linearly related to the square root of this ratio. The receptive field of tectal cells is composed of an excitatory center and an inhibitory periphery, and this periphery does not inhibit responses to looming stimuli. These results suggest that three classes of tectal neurons are specified for detecting an object approaching on a collision course towards the animal, and that rho and eta cells may signal early warning of impending collision whereas tau cells initiate avoidance responses at a constant time before collision through the tectopontine system.

Introduction

The optic tectum in non-mammals such as birds is the principal destination of retinal ganglion axons and sends output to the diencephalic nucleus rotundus (nRt), which in turn projects efferents in a topographic manner to the telencephalic entopallium (formerly named the ectostriatum) (Benowitz & Karten, 1976; Bischof & Watanabe, 1997; Deng & Rogers, 1998; Hellmann & Güntürkün, 2001; Reiner *et al*., 2004). This ascending tectofugal pathway is the most prominent visual pathway in non-mammals, which may be homologous to the colliculo-pulvinar-cortical pathway in mammals (Shimizu & Bowers, 1999; Nguyen *et al*., 2004). The non-mammalian tectum and its mammalian homolog, the superior colliculus, are involved in defensive behaviors (Grüsser & Grüsser-Cornehls, 1976; Ewert, 1984, 1997; Dean *et al*., 1989; Brandao *et al*., 1994), suggesting that tectal cells should be responsive to an object looming towards the animal. Electrophysiological evidence for the involvement of the tectofugal pathway in defensive responses has been obtained from experiments showing that rotundal cells in the pigeon can compute the optic variables of an object approaching on a direct collision course towards the animal, thereby allowing the bird to determine the time remaining to collision (Wang & Frost, 1992; Sun & Frost, 1998; Frost & Sun, 2003). Thus, we wanted to know whether tectal cells in the pigeon would detect an object looming towards the animal, and if so, whether this looming information would transmit to the nRt or to the tectopontine system that may be involved in avoidance responses (Hellmann *et al*., 2004).

It is known that looming-sensitive neurons in the pigeon nRt and in the locust visual system all possess a wide receptive field (Rind & Simmons, 1992, 1999; Hatsopoulos *et al*., 1995; Sun & Frost, 1998; Gabbiani *et al*., 1999; Frost & Sun, 2003), which is naturally thought to be suitable for detecting symmetrical expansion of the edge of a looming object. However, the excitatory receptive field (ERF) of tectal cells is generally smaller and surrounded by an inhibitory receptive field (IRF) (Jassik-Gerschenfeld & Guichard, 1972; Hughes & Pearlman, 1974; Frost *et al*., 1981; Gu *et al*., 2000; Wang *et al*., 2000), and therefore these cells do not seem to be appropriate for detecting a looming object. It is conceivable that the wide receptive field of looming detectors in the pigeon nRt results from a radial arrangement of concentric arrays of small tectal receptive fields (Frost & Sun, 2003). By contrast, tectal cells in layer 13 projecting to the nRt possess a wide dendritic field and high sensitivity to visual motion (Karten *et al*., 1997; Luksch *et al*., 1998; Marin *et al*., 2003). Some cells in the tectal layer 13 also project to the tectopontine system, which is involved in avoidance responses (Hellmann *et al*., 2004). This suggests that tectal neurons, prior to the nRt, may be able to detect a looming object and signal a predator or dangerous target approaching on a collision course. To examine this hypothesis, the present study recorded the response properties of tectal cells using extracellular recording and computer-aided mapping techniques.

Materials and methods

One hundred pigeons (*Columba livia*; body weight 340–440 g) were used. All experimental procedures followed guidelines for the care and use of animals established by the Society for Neuroscience. Each pigeon was anesthetized with urethane (20%, 1 mL/100 g) and then placed in a stereotaxic apparatus. The left tectum or caudal forebrain was exposed and the dura mater overlying the tectum or the nRt excised. The right eye was kept open, and the left eye covered. A screen of 130° vertical × 140°

Correspondence: Dr S.-R. Wang, as above.
E-mail: wangsr@sun5.ibp.ac.cn

Received 24 May 2005, revised 11 August 2005, accepted 24 August 2005

doi:10.1111/j.1460-9568.2005.04397.x

horizontal was placed 40 cm away from the viewing eye. The horizontal meridian of the visual field was rotated clockwise by 38° from the experimenter's view (Britto *et al*., 1990; Fu *et al*., 1998) to meet the pigeon's normal conditions (Erichsen *et al*., 1989).

Two kinds of visual stimuli were generated by a computer (X900PI4, Asus, Taiwan, China) with a graphics-card (Gforce 4 Ti 4600, MSI, Taiwan, China): (a) a black square of 4° (visual angle) that was moved along a series of parallel paths covering the whole screen for mapping the ERF and IRF of the recorded visual neurons (Fu *et al*., 1998) – in cells that were not spontaneously active, the IRF was plotted by lengthening a square stimulus (6 × 6°) up to 130° perpendicularly to its direction of motion (Frost *et al*., 1981; Yang *et al*., 2002); and (b) a soccer-ball-like pattern (diameter 10–80 cm) with alternating black and white panels of equal areas so that its overall luminance was unchanged when it was looming (Wang & Frost, 1992; Sun & Frost, 1998). In some experiments, a grey sphere and an annulus were also used. The luminance of black and white was 0.1 and 6.6 cd/m^2, respectively. The stimulus was projected with a projector (PJ550, ViewSonic Corp., CA, USA) onto the screen, and it first stayed stationary on the screen for 1000 ms to collect spontaneous spikes as controls, and was then presented with an interval of at least 5 s between trials to allow the cell to recover from any motion adaptation.

Visual cells were recorded extracellularly from the tectum, and for comparison some rotundal cells were also stereotaxically recorded (Karten & Hodos, 1967) with a micropipette (2 μm tip diameter, 10–15 MΩ impedance) filled with 2 M sodium acetate and 2% pontamine skyblue (Hellon, 1971; Gu *et al*., 2000). Neuronal spikes were conventionally amplified, displayed and fed into the computer for on-line analysis by averaging firing rates accumulated in 3–10 repeats. After a looming-sensitive neuron was isolated, the simulated object was moved on a direct collision course towards the pigeon's eye along a simulated path of 10–30 m (from the starting point of motion in depth to the eye) at a constant velocity, *v*, of 3–9 m/s. It stopped moving at the time determined by the simulated path length/the constant velocity at which the object was looming towards the eye, and this moment when the object virtually arrived at the eye (collision) was defined as the time-to-collision (T_c) and set to zero as the time reference. The response onset time of looming responses was measured relative to $T_c = 0$ in recording traces (Fig. 1) that were aligned with the time course of motion by the computer. The object did not necessarily subtend the whole screen at T_c because tectal ERFs are usually small and large IRFs did not respond to looming objects.

To examine whether looming-sensitive cells project from the tectum to the ascending tectorotundal pathway or to the ipsilateral tectopontine (ITP) and contralateral tectobulbar (CTB) pathways, a tungsten bipolar electrode was vertically inserted into the nRt, or horizontally into the lateral tegmental region of the formation reticularis lateralis mesencephali, or the medial tegmental region of the decussatio brachiorum conjunctivorum (Hellmann *et al*., 2004). Its poles were glass-coated, 400 μm apart and 60 μm at the tip was exposed. Rectangular pulses of 100–500 μA and 50–100 μs duration were applied. For recording electrocardiogram (ECG) to show cardioacceleration in response to looming stimulation, two stainless-steel needles were inserted into the bases of the pigeon's wings with the one contralateral to the heart as reference. ECG signals were amplified (DC to 200 Hz) and fed into the oscilloscope for display and a data recorder for off-line analysis. Heartbeats were accumulated in a time bin of 1 s and averaged in five repeats and then multiplied by 60 (in beats/min). These data were fitted by a Gaussian function with the software Origin (Version 7.5, OriginLab Corp., MA, USA). The onset of cardioacceleration was determined by the intersection point of an average heart rate recorded under control conditions with the Gaussian fitting to heart rates obtained under looming stimulation (see Fig. 7).

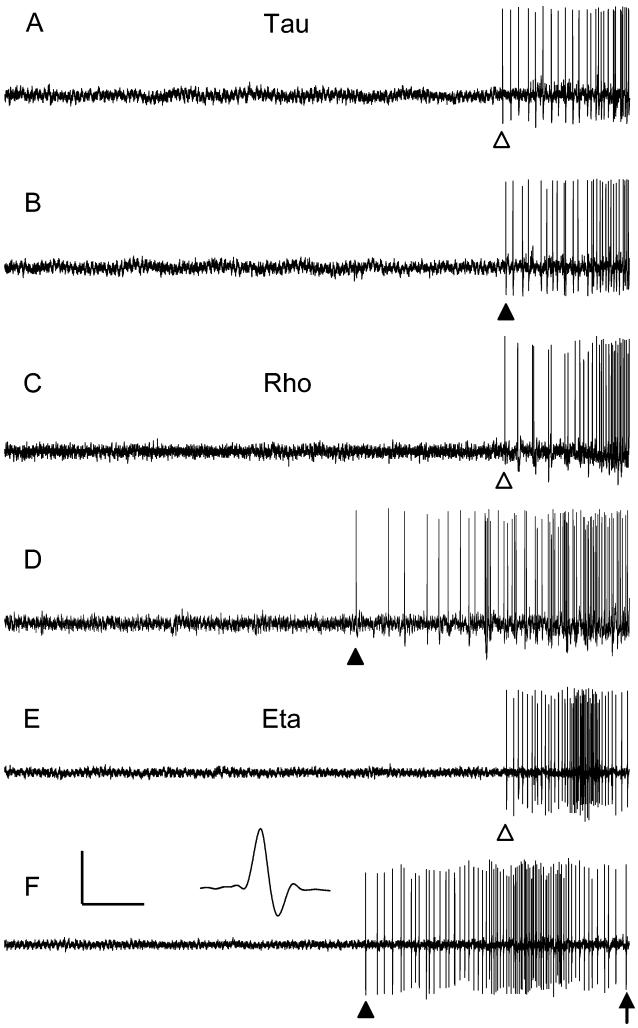

FIG. 1. Single-unit recordings made from tectal neurons responding to an object approaching on a collision course towards the pigeon. Recording traces show different responses of tau (A and B), rho (C and D) and eta (E, F) cells to an object 10 cm in diameter approaching at 3 m/s (A, C and E) and to an object 30 cm in diameter approaching at 3 m/s (B, D and F) towards the pigeon. Inset: the waveform of a tectal spike evoked by looming stimulus. Triangles indicate the onset of looming responses to small (△) and large (▲) objects. Upward arrow points to the time-to-collision. Scales bars: 300 ms (2 ms in inset) and 100 μV.

The recording sites of some looming-sensitive neurons in the tectum and nRt were marked with pontamine skyblue applied by negative current pulses of 10–20 μA and 0.5 s duration at 1 Hz for 10–15 min. Electrical stimulation sites in the nRt, ITP and CTB were marked by passing positive currents of 40 μA for 10 s through the active pole of bipolar electrodes. Under deep anesthesia, the brain was removed from the skull, fixed in 4% paraformaldehyde for 6–12 h and soaked in 30% sucrose solution in a refrigerator overnight. Frozen sections were cut at 40 μm thickness and counterstained with cresyl violet. Sections were dehydrated and covered for subsequent microscopic observation (Cao *et al*., 2004).

Results

The visual responses of 376 tectal neurons were recorded, of which 113 (30%) were looming-sensitive; those of 128 neurons were

recorded in the nRt, of which 36 (28%) were looming-sensitive. Rotundal cells were recorded for comparison with tectal cells. In some experiments, histological markings confirmed the recording sites of rotundal and tectal neurons.

Three classes of looming-sensitive neurons in the tectum

Single unit recordings were made from 376 tectal neurons, 113 of which (30%) responded to an object approaching on a collision course towards the pigeon. The rest of the cells did not respond to looming stimulation and thus were omitted from further analysis. All the looming-sensitive tectal cells started tonic firing at some time before collision but they were characterized by different firing patterns (Fig. 1). According to the physiological criteria used for classifying looming-sensitive cells in the nRt by Sun & Frost (1998), these looming-sensitive cells in the tectum were classified into tau, rho and eta cells based on their firing patterns to looming objects of different sizes and velocities. Tau cells (22/113, 19%) initiated firing at an approximately constant time, and their firing rates grew in an exponential fashion during approach of an object towards the eye and finally peaked at the moment when collision occurred (Figs 1A and B, and 2A–C). This firing pattern could be described by a mathematical formula $\tau(t) = \theta(t)/\theta'(t)$, where $\theta(t)$ is the angle subtended by the approaching object and $\theta'(t)$ is the rate at which the angle expands at a given time t. It appeared that the response onset time of tau cells was independent of the size and velocity of the looming object when velocity was constant and $\theta(t)$ values were low. The response onset time of these tectal tau cells was 650 ± 150 ms (mean ± SD, $n = 22$) before collision. By contrast, the firing patterns of rho cells (20/113, 18%) and eta cells (71/113, 63%) were similar in that both initiated an earlier firing to looming objects of larger sizes and lower velocities but different in that rho cells monotonically increased their firing rate until collision (Figs 1C and D, and 2D–F) whereas eta cells dropped off their firing rate after a peak was reached before collision (Figs 1E and F, and 2G–I). Rho cells computed the absolute rate of expansion of the looming object, and their firing pattern was best described by a formula $\rho(t) = \theta'(t)$. The firing pattern of eta cells was best described by a mathematical formula $\eta(t) = C \cdot \theta'(t)/e^{\alpha\theta(t)}$, where $\theta(t)$ is the angular size of the approaching object and $\theta'(t)$ is the change rate of $\theta(t)$, and C and α are constants for a given neuron. Figure 3 clearly shows that looming-sensitive cells in the pigeon tectum were distinctly classified into three groups: tau, rho and eta cells.

The response onset time of tectal tau cells should be longer than that of rotundal tau cells because the nRt is downstream of the the tectum, but the situation observed was just the opposite (650 ms in tectal cells in the present study vs. 1000 ms in rotundal cells reported by Wang & Frost, 1992). To resolve the cause of this discrepancy, 36

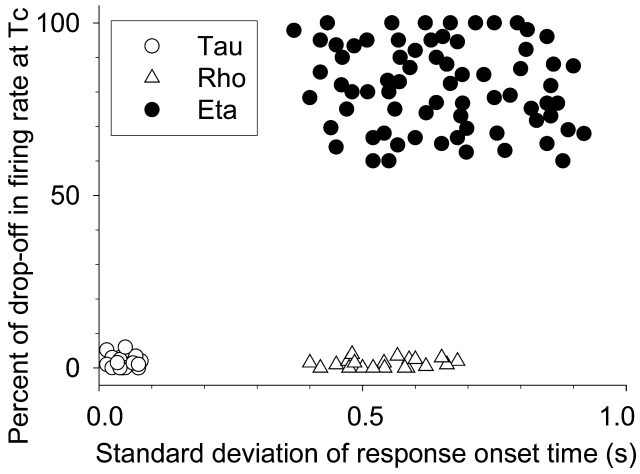

FIG. 3. Classification of looming-sensitive cells in the pigeon tectum into three groups according to their response properties. The ordinate represents the percentage decrease in firing rate to an object 30 cm in diameter moving at 3 m/s at the time-to-collision (T_c), which is calculated by the formula $(f_p - f_{tc})/(f_p - f_s)$ where f_p, f_{tc} and f_s are the peak firing rate, firing rate at T_c and spontaneous rate, respectively, and the abscissa represents the standard deviation of the response onset time relative to T_c, which is obtained by calculating the response onset time of these cells to objects 10 cm and 30 cm in diameter moving at 3 m/s and 9 m/s.

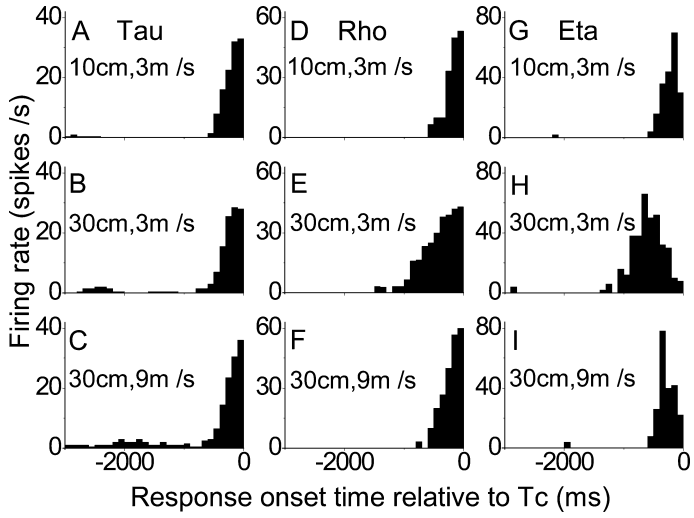

FIG. 2. Histograms showing the firing patterns of three classes of tectal neurons responding to objects approaching on a collision course towards the pigeon. Tau cells (A–C) initiated firing at an approximately constant time before collision regardless of the size (10 or 30 cm in diameter) and velocity (3 or 9 m/s) of looming objects. Rho (D–F) and eta (G–I) cells started earlier firings to larger and/or slower-moving objects (E and H) and were different in that the firing rate of eta cells increased to a peak and then dropped off until the time-to-collision (T_c). Three repeats were averaged. Negative values indicate the time before collision. Time bin, 100 ms.

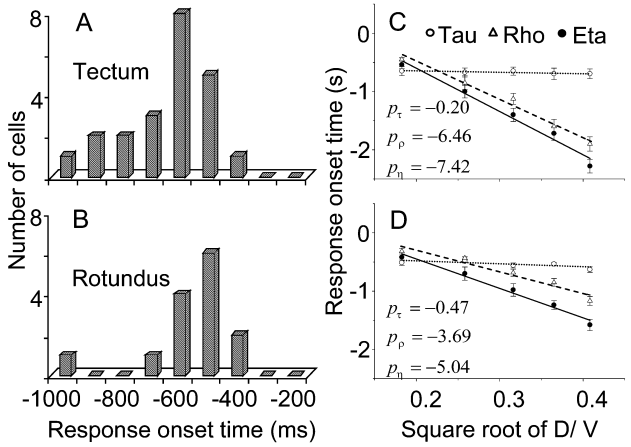

FIG. 4. Relationship between the response onset time of three classes of looming-sensitive cells and the physical parameters of looming objects in the optic tectum (A and C) and the nucleus rotundus (B and D). Tau cells initiated firing at an average of 650 ms before collision for tectal cells (A, $n = 22$) and 560 ms for rotundal cells (B, $n = 14$) regardless of the size and velocity of objects. The response onset time of rho and eta cells in both structures is linearly related to the square root of the diameter/velocity ratio of looming objects (C and D). The slopes (p) of the linearly fitted lines for tectal (C) and rotundal (D) cells are shown with suffixes identifying tau, rho and eta cells. Five diameter/velocity (D/V) ratios were examined for each of five cells whose response onset time was averaged. Negative values indicate the time before collision. Error bars represent ± SEM.

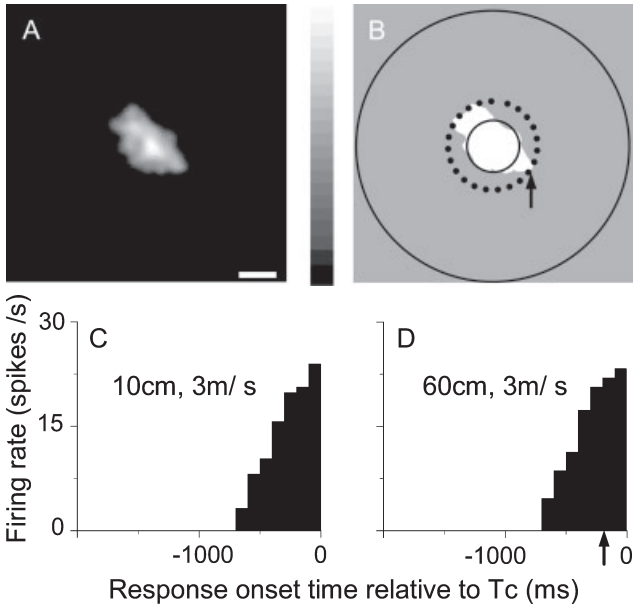

FIG. 5. Inhibitory receptive field in a tectal cell did not suppress its looming responses. The receptive field mapped by the computer of this tau cell was composed of an ERF (white) and an IRF (black) (A), both of which were depicted (B, IRF in grey) showing that firing pattern (C) evoked by a small soccer ball (diameter = 10 cm) was identical to that (D) by a large soccer ball ($d = 60$ cm) looming at 3 m/s towards the animal. Small and large circles (B) represent the final position where the small and large object 'collided' with the animal, respectively. The dashed circle symbolizes the position of the edges of the large object just completely expanding into the IRF (arrow), and the firing rate continuously increased (arrow) to a peak at the time-to-collision = zero. Scale bar, 10°, and the grey scale represents 0–20 spikes/s (A). Five repeats were averaged, negative values indicate the time before collision, and time bin, 100 ms.

looming-sensitive cells out of the 128 rotundal cells (36/128, 28%) were examined. They included 14 tau cells (39%), 12 rho cells (33%) and 10 eta cells (28%). The response onset time of rotundal tau cells averaged 560 ± 150 ms ($n = 14$). The response onset time of tectal tau cells apparently matched that of rotundal tau cells in the present study. By contrast, rotundal rho and eta cells were similar to tectal rho and eta cells in that their response onset time was linearly related to the square root of the diameter/velocity ratio of looming objects but different in that their dependence was weaker than for tectal cells (Fig. 4C and D). The slopes of the relationship were 3.69 for rho cells and 5.04 for eta cells in the nRt, significantly smaller than the values for rho (6.46) and eta (7.42) cells in the tectum, respectively, indicating that tectal rho and eta cells initiated an earlier firing than rotundal rho and eta cells in response to looming objects with the same ratio of diameter to velocity.

Inhibitory receptive fields do not suppress looming responses

Although these tectal cells computed different optic variables of an object looming on a collision course with the animal, their receptive fields all comprised an ERF surrounded by an IRF. The ERF of 55 looming-sensitive cells was mapped using translating bars and the IRF was obtained by gradually lengthening this stimulus (see Methods). The size of the ERF and IRF was measured by averaging their longest and shortest dimensions. The ERF extent of these cells ranged from 10 to 56° with an average of 30 ± 11°, and the IRF was about 2–8 times larger than the ERF. Interestingly, this wide IRF did not influence the firing rate and pattern of tectal looming-sensitive cells. Figure 5 gives an example showing that the IRF of a tectal tau cell did not suppress its visual responses to looming stimuli. The ERF of this cell was mapped with the computer and the IRF was determined by gradually lengthening the stimulus because this cell was not spontaneously active. The firing pattern evoked by a small soccer ball (diameter $d = 10$ cm) approaching at 3 m/s only within the ERF (Fig. 5B and C) was identical to that evoked by a large soccer ball ($d = 60$ cm) moving at 3 m/s into the IRF (Fig. 5B and D), characterized by the fact that the response onset time was 700 ms before collision and average firing rate was 15 spikes/s to either of the small and large soccer balls, and the peak firing rate was 24 spikes/s to the small soccer ball and 23 spikes/s to the large one. This IRF also did not affect the visual responses of looming cells to a grey sphere ($d = 60$ cm) looming at 3 m/s on a collision course toward the animal. However, looming-sensitive cells stopped firing at the moment when the edges of an annulus ($d = 60$ cm) were expanding into the IRF. By contrast, any visual stimulus motion through the IRF on the screen plane evoked strong inhibition in this cell.

Tectal looming cells project to the tectorotundal and tectopontine systems

It is known that the tectum sends efferents in the ascending tectorotundal pathway and in the descending tectopontine and tectobulbar pathways. To determine whether tectal looming cells send efferents in these pathways, electrical stimulation was applied to examine antidromic activation in 42 tectal cells, including five tau cells, seven rho cells and 30 eta cells. Supra-threshold stimulation (300–500 μA, 50–100 μs) to the ITP evoked antidromic spikes in five (12%) tectal looming cells with an average latency of 1.8 ± 0.7 ms (Fig. 6A and B). Rotundal stimulation evoked antidromic spikes in 13 (31%) tectal looming cells with an average latency of 2.5 ± 0.7 ms (Fig. 6C and D). One electrical shock evoked one antidromic spike in

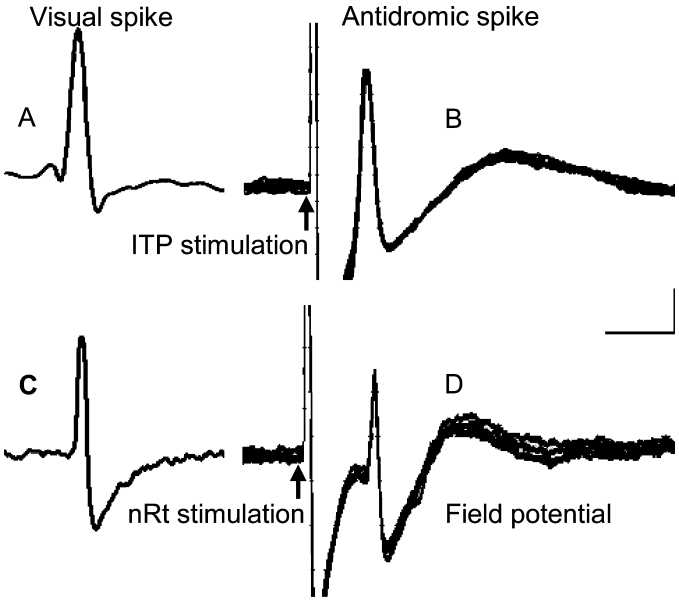

FIG. 6. Looming-sensitive tectal neurons project to the nucleus rotundus (nRt) and the tectopontine system (ITP). Electrical stimulation (350–500 μA in intensity, 100 μs in duration) of the ITP and nRt evoked antidromic spikes in two tectal eta cells (A and B, C and D). Visual spikes evoked by looming stimulation in A and C are similar in amplitude and waveform to antidromic spikes in B and D, respectively. Six repeats were superimposed in B and D. Upward arrows point to electrical stimulation artifacts. Scale bars: 80 μV (A and B); 50 μV (C and D); and 2 ms (A–D).

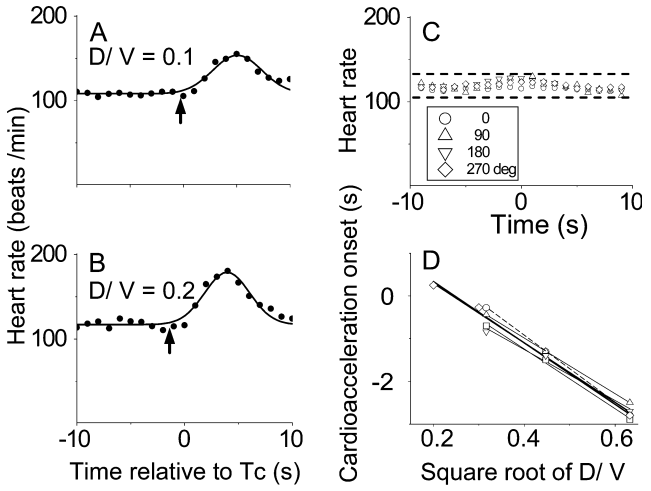

FIG. 7. Heart rate increased as an object approached on a collision course towards the pigeon. Cardioacceleration onset (arrow) was advanced from 0.28 s to 1.31 s before the time-to-collision (T_c) and peak rate increased from 154 to 179 beats/min as the diameter/velocity ratio (D/V) of objects increased from 0.1 (d = 50 cm, v = 5 m/s) to 0.2 (d = 60 cm, v = 3 m/s) (A, B). Planar motion of these objects on the screen in the horizontal and vertical directions did not alter the heart rate (C). Statistical data from five pigeons (different symbols) showed that cardioacceleration onset was linearly related to the square root of the diameter/velocity ratio (D), with an average slope of 6.97. Negative values indicate the time before collision (A, B and D) or before the object's arrival at the screen centre (C).

the tectal looming cells projecting to the nRt or ITP. The similarity of the antidromic spikes to the visual spikes in amplitude and waveform indicated that both spikes were recorded from the same tectal cells (Fig. 6A–D). None of these tectal cells was antidromically activated by both the ITP and the nRt stimulations. Whether tectal looming cells project to the CTB was examined in an additional nine tectal cells, including two tau and seven eta cells; none was activated by electrical stimulation to this descending pathway.

Relationship between looming-sensitive cells and cardioacceleration

An object approaching on a direct collision course towards the animal signals an impending danger, which would result in an increase in heart rate of the animal. The pigeon's heart rate was accelerated by looming objects (Fig. 7A and B) but not by motion of these objects on the screen plane (Fig. 7C). It appeared that the cardioacceleration onset was earlier and the peak heart rate was higher as the diameter/velocity ratio of looming objects became larger. For example, the pigeons detailed in Fig. 7A–C had an average heart rate of 120 beats/min as controls, and this rate began to increase at 0.28 s before collision and peaked to 154 beats/min at 4.92 s after collision when the diameter/velocity ratio was 0.1, whereas the rate increased at 1.31 s before collision and peaked to 179 beats/min at 3.75 s after collision when the ratio was 0.2. However, motion of these objects in four orthogonal directions (nasal-0, 90, 180 and 270°) on the screen plane did not accelerate the heart rate. The onset time of cardioacceleration relative to T_c was linearly related to the square root of the diameter/velocity ratio of looming objects, with an average slope of 6.97 obtained from five pigeons (Fig. 7D). This value was close to the slopes for tectal rho and eta cells but deviated from those of rotundal rho and eta cells (Fig. 4C and D). It implied that visual information signaled by tectal rho and eta cells may be responsible for early warning of an impending object whereas tau cells may signal a predator or dangerous object at a constant time before collision and initiate avoidance responses through the tectopontine system.

Recording and stimulation sites

The recording sites of 26 tectal looming-sensitive cells (eight tau, three rho and 15 eta cells) were marked with dye and all of them were localized in the tectal layer 13. Of these tectal cells, two projected to the ITP and one to the nRt, as demonstrated by antidromic activation. Three stimulation sites putatively in the nRt, two sites in the ITP and two sites in the CTB were marked by electrolytic lesions, and all of them were localized within these structures. The recording sites of 14 rotundal looming cells (seven tau, two rho and five eta cells) were marked with dye, and they were all localized within the nRt, with a preferential distribution in the dorsal part of the nucleus.

Discussion

The present study found that a subpopulation of visual neurons in the pigeon tectum respond to an object approaching on a collision course towards the animal. Previous studies (Wang & Frost, 1992) did not find looming-sensitive cells in the pigeon optic tectum probably because they did not record enough tectal cells in layer 13 where looming-sensitive cells are located (as found in the present study). Our finding lends strong support to the notion that the non-mammalian tectum and the superior colliculus in mammals are involved in defensive movements (Grüsser & Grüsser-Cornehls, 1976; Ewert, 1984, 1997; Dean *et al.*, 1989; Brandao *et al.*, 1994). Two lines of evidence indicate that the visual responses of these tectal neurons are evoked by symmetrical expansion of an object approaching on a direct

collision course towards the animal but not by lateral motion of the object edges on the screen plane. First, any two-dimensional motion on the screen plane does not enhance the heart rate of pigeons whereas motion of an object looming towards the animal certainly does. Both the response onset time of tectal rho and eta cells and the cardioacceleration onset time of pigeons are linearly related to the square root of the diameter/velocity ratio of looming objects. Second, any planar motion of an object elicits excitatory responses in the ERF and inhibitory responses in the IRF of tectal cells, whereas symmetrical expansion of the edges of a looming object within the IRF cannot inhibit visual responses in tectal cells sensitive to looming stimuli.

According to the physiological criteria for classifying looming-sensitive cells in the nRt (Sun & Frost, 1998), these tectal cells are grouped into tau, rho and eta cells, the computations of which are the same as those of rotundal tau, rho and eta cells, respectively. The recording sites marked with dye indicate that these looming cells are all localized in tectal layer 13. Tectal ganglion cells in this layer possess a wide dendritic field and high sensitivity to motion over many dendritic bottlebrushes (Karten *et al*., 1997; Luksch *et al*., 1998; Marin *et al*., 2003), and therefore they may be able to detect symmetrical expansion of a looming object. Tectal neurons in layer 13 project axons to the nRt in the tectorotundal pathway (Karten *et al*., 1997; Luksch *et al*., 1998; Marin *et al*., 2003; Hellmann *et al*., 2004), as well as to the tectopontine and the tectobulbar pathways (Hellmann *et al*., 2004). Antidromic activation shows that about 30% of tectal looming cells project to the nRt and 10% of tectal looming cells project to premotor hindbrain regions in the tectopontine system. Therefore, looming information can directly initiate avoidance behaviors in an animal facing an impending collision. It is likely that looming-sensitive cells in tectal layer 13 do not project to the tectobulbar pathway as this pathway may not be involved in avoidance behaviors (Hellmann *et al*., 2004).

It appears that looming information in the nRt directly originates, at least in part, from tectal looming-sensitive cells. However, the possibility that looming detectors in the pigeon nRt are organized from radial arrangements of concentric arrays of small-field local motion detectors in the optic tectum cannot be excluded (Frost & Sun, 2003). The fact that the remaining 60% of tectal looming cells were found to project to neither the nRt nor the ITP could be explained in two ways: (1) some stimulation electrodes in the nRt or the ITP might not be placed at sites correctly corresponding to the recorded neurons; and (2) some of these tectal cells may project to neuronal structures other than the nRt and the ITP.

The response onset time for tectal tau cells is 650 ms whereas that for rotundal tau cells is 560 ms before collision. This difference in response onset time is due to the fact that the nRt is downstream of the tectum. The response onset time of tau cells in the pigeon is similar to that of the lobula giant movement detectors in the locust, which respond when an impending collision is 200–400 ms away (Rind & Simmons, 1999). However, the response onset time of rotundal tau cells obtained in the present study is different from that reported previously (Wang & Frost, 1992; Sun & Frost, 1998). This discrepancy is most likely due to differences in determining T_c. Unfortunately, the previous studies did not specify how this key parameter was defined. It appears that these authors defined T_c as the time when the object subtended the whole screen rather than the time determined by the simulated path length/the constant velocity of looming motion. The fact that the firing rate at T_c is smaller than the peak rate for tau cells (see fig. 2 in Sun & Frost, 1998) may suggest this possibility because the firing rate of tau cells at T_c should be at or close to the peak, as shown in Fig. 2. Therefore, T_c may be postponed until after collision has almost occurred according to the time course of motion. In addition, single-unit recordings should be precisely aligned on-line with the time course of motion; the transfer of data from the collecting system to a computer for processing histograms (Wang *et al*., 1993) may also delay T_c.

It is interesting to note that the response onset time of tectal tau cells is approximately constant regardless of the size and velocity of looming objects, whereas that of rho and eta cells is linearly related to the square root of the diameter/velocity ratio of looming objects (Fig. 4C and D). However, the cardioacceleration onset relative to T_c is also linearly related to this value (Fig. 7D). Furthermore, the slope of cardioacceleration (Fig. 7D) approximates to the slopes for the response onset time of tectal rho and eta cells but deviates from those for rotundal rho and eta cells (Fig. 4C and D). These results suggest that the tectum may play a more important role than the nRt in signaling collision, and that tectal rho and eta cells probably give an early warning of an impending object whereas tectal tau cells signal a predator or dangerous object at a constant time before collision and thus initiate avoiding and escaping responses through the tectopontine system.

Acknowledgements

This work was supported by the National Natural Science Foundation of China (Grant no. 90208008) and by the Brain–Mind project of the Chinese Academy of Sciences.

Abbreviations

CTB, contralateral tectobulbar pathway; ECG, electrocardiogram; ERF, excitatory receptive field; IRF, inhibitory receptive field; ITP, ipsilateral tectopontine pathway; nRt, nucleus rotundus; T_c, time-to-collision.

References

Benowitz, L.I. & Karten, H.J. (1976) Organization of the tectofugal visual pathway in the pigeon: a retrograde transport study. *J. Comp. Neurol.*, **167**, 503–520.

Bischof, H.J. & Watanabe, S. (1997) On the structure and function of the tectofugal visual pathway in laterally eyed birds. *Eur. J. Morphol.*, **35**, 246–254.

Brandao, M.L., Cardoso, S.H., Melo, L.L., Motta, V. & Coimbra, N.C. (1994) Neural substrate of defensive behavior in the midbrain tectum. *Neurosci. Biobehav. Rev.*, **18**, 339–346.

Britto, L.R., Gasparotto, O.C. & Hamassaki, D.E. (1990) Visual telencephalon modulates directional selectivity of accessory optic neurons in pigeons. *Vis. Neurosci.*, **4**, 3–10.

Cao, P., Gu, Y. & Wang, S.R. (2004) Visual neurons in the pigeon brain encode the acceleration of stimulus motion. *J. Neurosci.*, **24**, 7690–7698.

Dean, P., Redgrave, P. & Westby, G.W. (1989) Event or emergency? Two response systems in the mammalian superior colliculus. *Trends Neurosci.*, **12**, 137–147.

Deng, C. & Rogers, L.J. (1998) Organization of the tectorotundal and SP/IPS-rotundal projections in the chick. *J. Comp. Neurol.*, **394**, 171–185.

Erichsen, J.T., Hodos, W., Evinger, C., Bessette, B.B. & Phillips, S.J. (1989) Head orientation in pigeon: postral, locomotor and visual determinants. *Brain Behav. Evol.*, **33**, 268–278.

Ewert, J.P. (1984) Tectal mechanisms that underlie prey-catching and avoidance behaviours in toads. In Vanegas, H. (Ed.), *Comparative Neurology of the Optic Tectum*. Plenum Press, New York, pp. 247–416.

Ewert, J.P. (1997) Neural correlates of key stimulus and releasing mechanism: a case study and two concepts. *Trends Neurosci.*, **20**, 332–339.

Frost, B.J., Scilley, P.L. & Wong, S.C.P. (1981) Moving background patterns reveal double-opponency of directionally specific pigeon tectal neurons. *Exp. Brain Res.*, **43**, 173–185.

Frost, B.J. & Sun, H.J. (2003) The biological bases of time-to-collision computation. In Hecht, H. & Savelsbergh, G.J.P. (Eds), *Time-to-Contact, Advances in Psychology Series*. Elsevier, Amsterdam, pp. 13–38.

Fu, Y.X., Gao, H.F., Guo, M.W. & Wang, S.R. (1998) Receptive field properties of visual neurons in the avian nucleus lentiformis mesencephali. *Exp. Brain Res.*, **118**, 279–285.

Gabbiani, F., Krapp, H.G. & Laurent, G. (1999) Computation of object approach by a wide-field, motion-sensitive neuron. *J. Neurosci.*, **19**, 1122–1141.

Grüsser, O.J. & Grüsser-Cornehls, U. (1976) Neurophysiology of the anuran visual system. In Llinas, R. & Precht, W. (Eds), *Frog Neurobiology.* Plenum Press, New York, pp. 297–385.

Gu, Y., Wang, Y. & Wang, S.R. (2000) Regional variation in receptive field properties of tectal cells in pigeons. *Brain Behav. Evol.*, **55**, 221–228.

Hatsopoulos, N., Gabbiani, F. & Laurent, G. (1995) Elementary computation of object approach by a wide-field visual neuron. *Science*, **270**, 1000–1003.

Hellmann, B. & Güntürkün, O. (2001) Structural organization of parallel information processing within the tectofugal visual system of the pigeon. *J. Comp. Neurol.*, **429**, 94–112.

Hellmann, B., Güntürkün, O. & Manns, M. (2004) Tectal mosaic: organization of the descending tectal projections in comparison to the ascending tectofugal pathway in the pigeon. *J. Comp. Neurol.*, **472**, 395–410.

Hellon, R.F. (1971) The marking of electrode tip positions in nervous tissue. *J. Physiol. (Lond.)*, **214**, 12.

Hughes, C.P. & Pearlman, A.L. (1974) Single unit receptive fields and the cellular layers of the pigeon optic tectum. *Brain Res.*, **80**, 365–377.

Jassik-Gerschenfeld, D. & Guichard, J. (1972) Visual receptive fields of single cells in the pigeon's optic tectum. *Brain Res.*, **40**, 303–317.

Karten, H.J., Cox, K. & Mpodozis, J. (1997) Two distinct populations of tectal neurons have unique connections within the retinotectorotundal pathway of the pigeon (*Columba livia*). *J. Comp. Neurol.*, **387**, 449–465.

Karten, H.J. & Hodos, W. (1967) *A Stereotaxic Atlas of the Brain of the Pigeon (Columba livia)*. Johns Hopkins Press, Baltimore.

Luksch, H., Cox, K. & Karten, H.J. (1998) Bottlebrush dendritic endings and large dendritic fields: motion-detecting neurons in the tectofugal pathway. *J. Comp. Neurol.*, **396**, 399–414.

Marin, G., Letelier, J.C., Henny, P., Sentis, E., Farfan, G., Fredes, F., Pohl, N., Karten, H.J. & Mpodozis, J. (2003) Spatial organization of the pigeon tectorotundal pathway: an interdigitating topographic arrangement. *J. Comp. Neurol.*, **458**, 361–380.

Nguyen, A.P., Spetch, M.L., Crowder, N.A., Winship, I.R., Hurd, P.L. & Wylie, D.R. (2004) A dissociation of motion and spatial-pattern vision in the avian telencephalon: implications for the evolution of 'visual streams'. *J. Neurosci.*, **24**, 4962–4970.

Reiner, A., Perkel, D.J., Bruce, A.B., Csillag, A., Kuenzel, W., Medina, L., Paxinos, G., Shimizu, T., Striedter, G., Wild, M., Ball, G.F., Durand, S., Gunturkun, O., Lee, D.W., Mello, C.V., Powers, A., White, S.A., Hough, G., Kubikova, L., Smulders, T.V., Wada, K., Dugas-Ford, J., Husband, S., Yamamoto, K., Yu, J., Siang, C. & Jarvis, E.D. (2004) Revised nomenclature for avian telencephalon and some related brainstem nuclei. *J. Comp. Neurol.*, **473**, 377–414.

Rind, F.C. & Simmons, P.J. (1992) Orthopteran DCMD neuron: a reevaluation of responses to moving objects. I. Selective responses to approaching objects. *J. Neurophysiol.*, **68**, 1654–1666.

Rind, F.C. & Simmons, P.J. (1999) Seeing what is coming: building collision-sensitive neurons. *Trends Neurosci.*, **22**, 215–220.

Shimizu, T. & Bowers, A.N. (1999) Visual circuits of the avian telencephalon: evolutionary implications. *Behav. Brain Res.*, **98**, 183–191.

Sun, H.J. & Frost, B.J. (1998) Computation of different optical variables of looming objects in pigeon nucleus rotundus neurons. *Nat. Neurosci.*, **1**, 296–303.

Wang, Y.C. & Frost, B.J. (1992) 'Time to collision' is signaled by neurons in the nucleus rotundus of pigeon. *Nature*, **356**, 236–238.

Wang, Y.C., Jiang, S.Y. & Frost, B.J. (1993) Visual processing in pigeon nucleus rotundus: luminance, color, motion, and looming subdivisions. *Vis. Neurosci.*, **10**, 21–30.

Wang, Y., Xiao, J. & Wang, S.R. (2000) Excitatory and inhibitory receptive fields of tectal cells are differentially modified by magnocellular and parvocellular divisions of the pigeon nucleus isthmi. *J. Comp. Physiol. A*, **186**, 505–511.

Yang, J., Li, X. & Wang, S.R. (2002) Receptive field organization and response properties of visual neurons in the pigeon nucleus semilunaris. *Neurosci. Lett.*, **331**, 179–182.